The Tasmantid Seamounts: A window into structural inheritance of ocean floor fabric

V21A-3034

Fred Richards[1,2*], Lara Kalnins[3], Tony Watts[1], Benjamin Cohen[4] & Robin Beaman[5]

[1]Department of Earth Sciences, University of Oxford, Oxford, UK [2]Bullard Laboratories, Department of Earth Sciences, University of Cambridge, Cambridge, UK [3]Department of Earth Sciences, Durham University, UK
[4]Scottish Universities Environmental Research Centre, East Kilbride, UK [5]College of Science, Technology and Engineering, James Cook University, Cairns, Australia

*fdr22@cam.ac.uk

1 Introduction

The Tasmantid Seamounts extend for >2000 km off the east coast of Australia, constituting one of three contemporaneous, sub-parallel Cenozoic hotspot tracks that traverse the region, locally separated by ≤500 km (Cohen *et al*., 2013). The seamounts young north to south, spanning ~50 - 6 Ma (McDougall & Duncan 1988; Kalnins *et al*., 2015).

At multiple locations, the Tasmantid chain intersects the extinct slow-spreading Tasman Sea ridge system, which was active between 84 - 53 Ma (Müller *et al*., 2008). Despite the >20 Ma hiatus between spreading cessation and seamount emplacement, palaeo-ridge structure appears to exert significant control on seamount morphology and structure.

Geophysical datasets acquired on voyage *ss2012_v07* have been analysed to answer the following:

1. What mechanism can account for the morphological diversity of the seamounts?
2. What is the relationship between pre-existing tectonic fabric, intraplate magmatism and the strength of the Tasman Sea lithosphere?
3. How has the strength of the Tasmantid melting anomaly evolved through time?

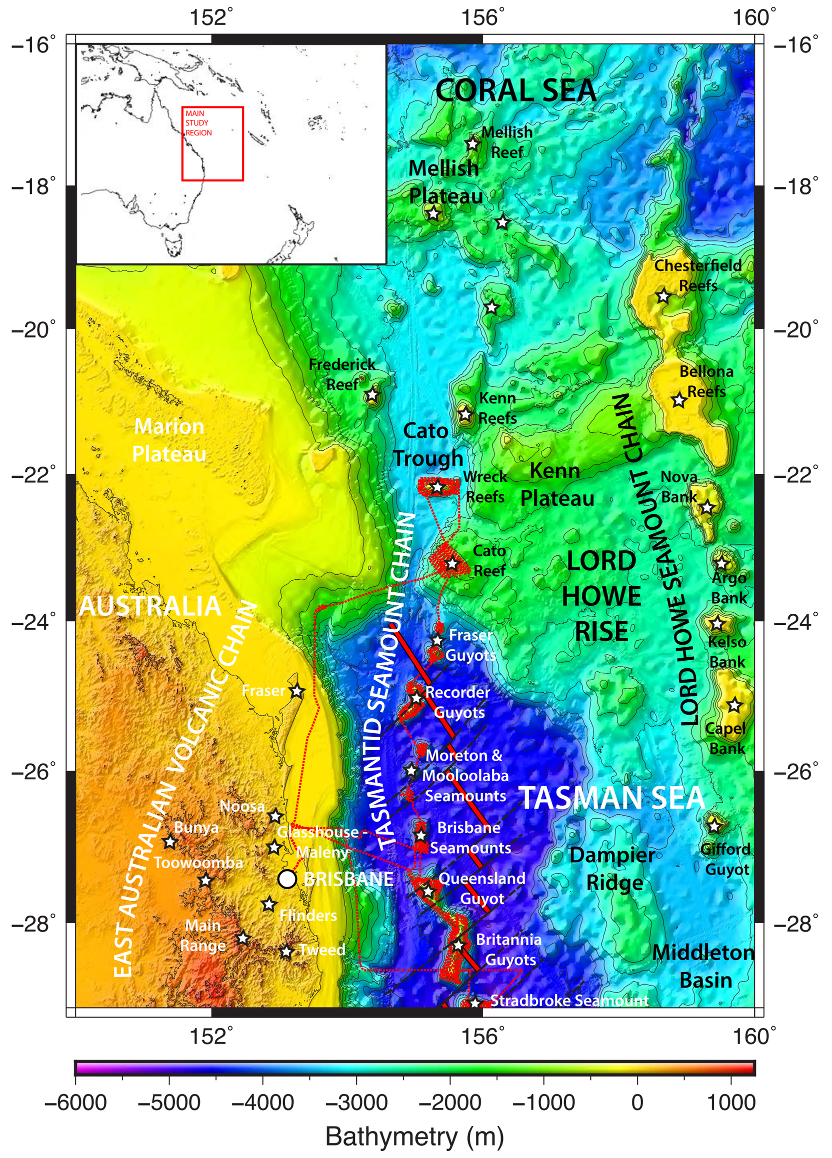

Figure 1. Map of the study area. Dotted red line = shiptrack of voyage *ss2012_v07*. Star = position of Cenozoic seamounts and volcanoes. Solid red line = extinct ridge axis, solid black line = transform fault, dashed black = fracture zone. Bathymetry derived from GBR100 dataset (Beaman 2010).

2 Volcanic Architecture

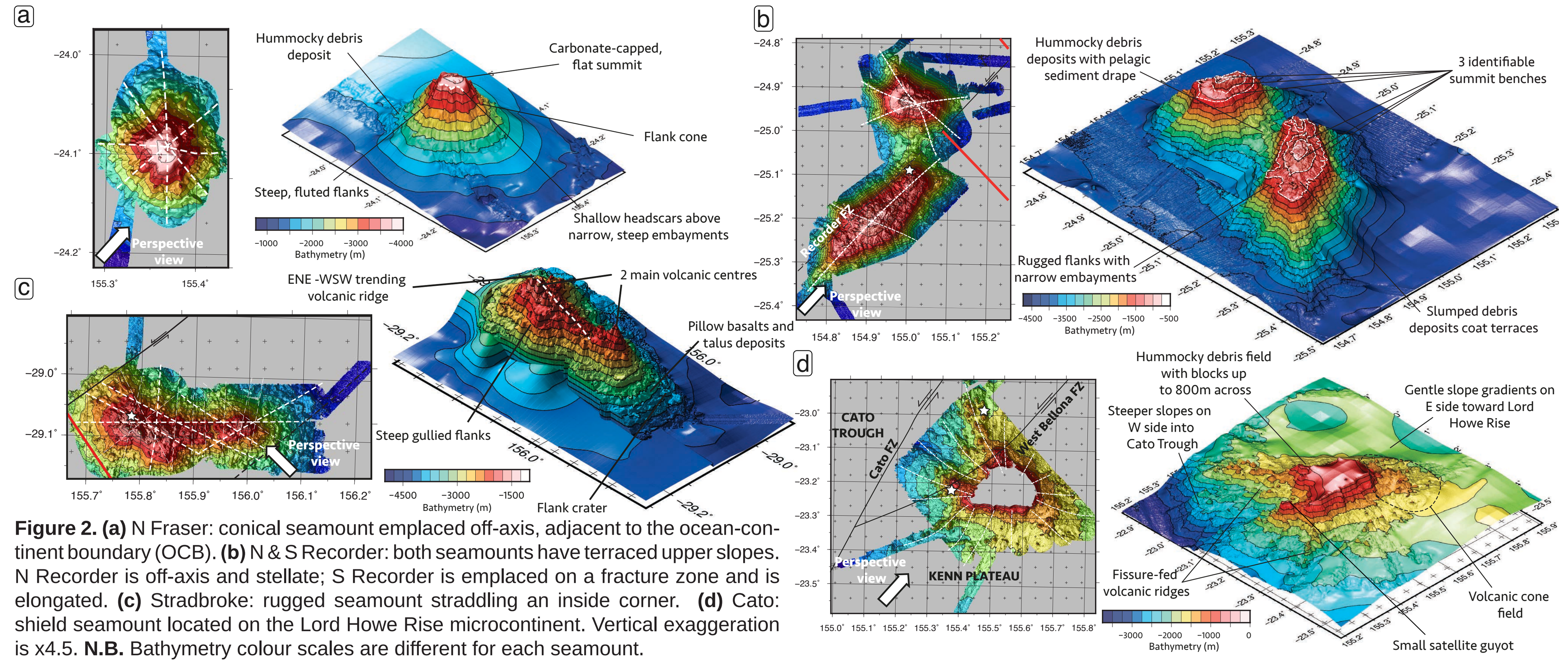

Figure 2. (a) N Fraser: conical seamount emplaced off-axis, adjacent to the ocean-continent boundary (OCB). **(b)** N & S Recorder: both seamounts have terraced upper slopes. N Recorder is off-axis and stellate; S Recorder is emplaced on a fracture zone and is elongated. **(c)** Stradbroke: rugged seamount straddling an inside corner. **(d)** Cato: shield seamount located on the Lord Howe Rise microcontinent. Vertical exaggeration is x4.5. **N.B.** Bathymetry colour scales are different for each seamount.

- Tasmantid morphologies fall into four distinct categories: a) conical seamounts characterised by steep, smooth flanks; b) elongate and stellate terraced seamounts with subaerially eroded peaks; c) rugged seamounts constructed via repeated fissure eruptions along crosscutting volcanic rift zones (VRZs) and d) shield seamounts with shallow slopes and dispersed cinder cones.
- The chain exhibits low mass wasting rates and fluctuating edifice volume, with dramatic morphological variation between seamounts separated by ≤10 km.
- There is a clear link between overall morphology and seamount position relative to the extinct spreading centre.

3 Slope Analysis

- Tectonic setting exerts major control on slope characteristics: conical seamounts with elevated slope gradients but lower inter-sector variance occur off-axis and at outside corners; rugged seamounts with low slope gradient but high inter-sector variability occur at inside corners.
- Terraced and shield seamounts have notably variable, low gradient upper slopes suggesting elevated rates of mass wasting due to sub-aerial exposure.
- The relatively low slope variance and elevated backscatter on the lower sections of the edifices indicate that large mass-wasting events are rare. This is consistent with minimal shallow deformation and may reflect modest eruption rate with a high intrusive-to-extrusive magmatic budget (Ramalho *et al*., 2013).

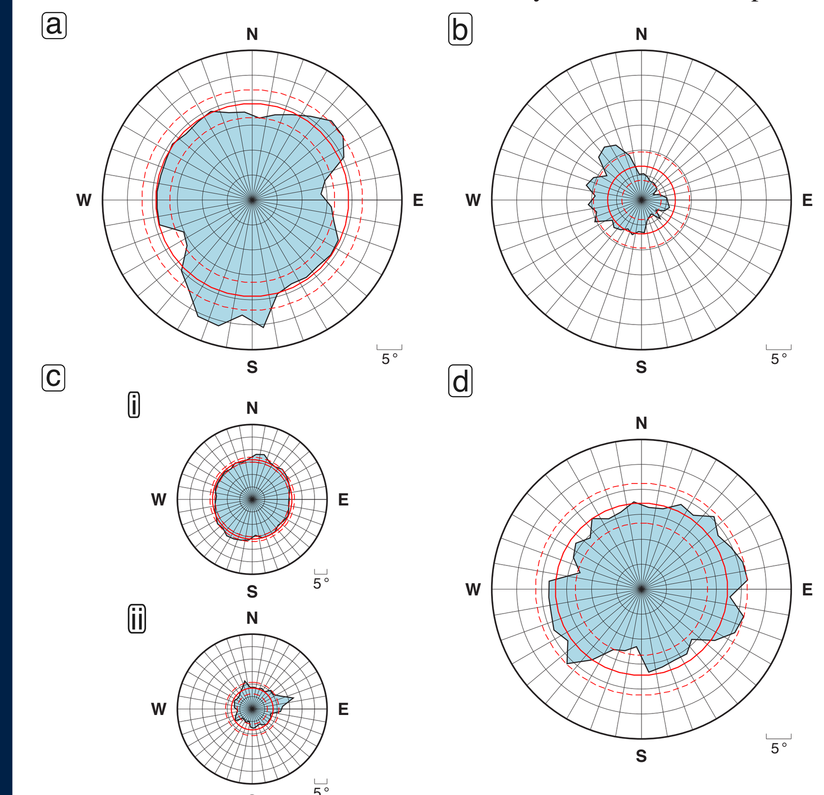

Figure 3. Average slope gradient by sector. **(a)** South Moreton, a conical seamount. **(b)** Cato, a shield seamount. **(c)** Britannia, a terraced seamount: **(i)** basal and **(ii)** upper, subaerially-eroded slopes. **(d)** Stradbroke, a rugged seamount.

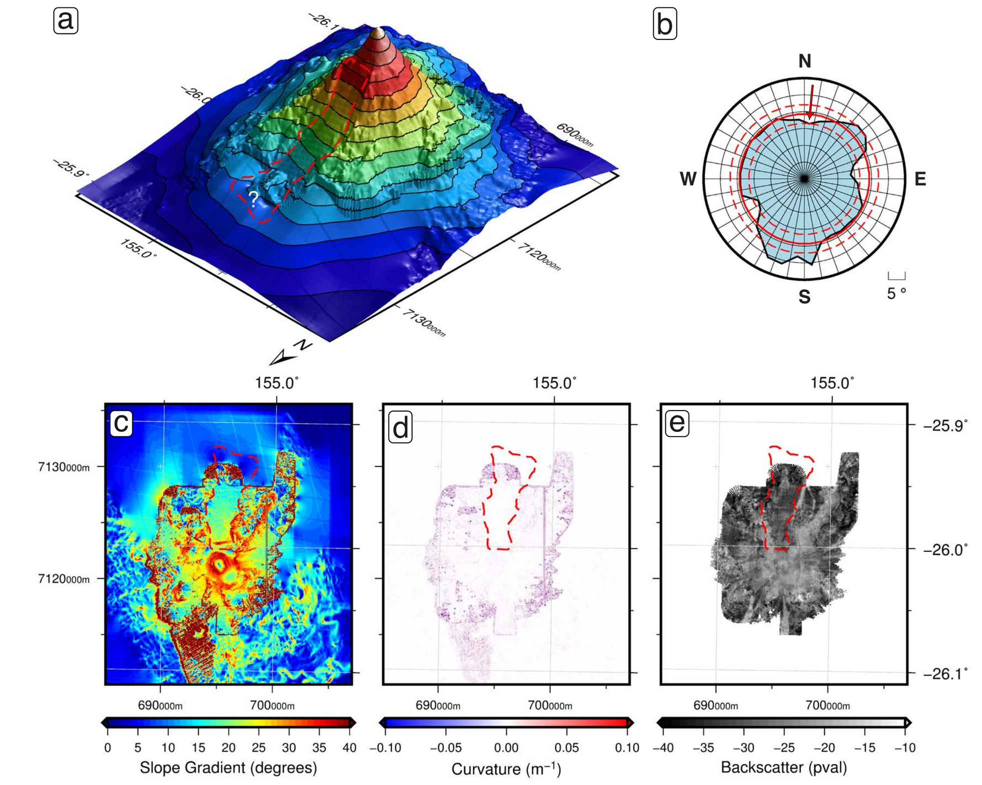

Figure 4. Detecting mass wasting. **(a)** SE-ward view of S Moreton, red dashes = mass wasting deposit with reduced mean slope gradient **(b)** and low backscatter **(e)**. Slope gradient is fairly constant **(c)** so bathymetric curvature **(e)** is ~ 0. The run-out distance: headscar aspect ratio suggests a debris avalanche mechanism (Mitchell *et al*., 2002).

4 Structural Orientations

Figure 5. Linear feature orientation vs. tectonic setting. **(a)** Stradbroke: **(i)** trends oblique-to-spreading; **(ii)** inside-corner setting. **(b)** S & N Recorder: **(i)** S Recorder: volcanic trends parallel to Fracture Zone and **(iii)** fracture zone setting **(ii)** N Recorder has ridge-parallel features and **(iii)** off-axis setting. **(c)** N Fraser: **(i)** trends ridge-parallel or subparallel to fracture zones; **(ii)** ocean-continent boundary setting. Red = major VRZs, blue = minor VRZs and black = faults. IC = inside corner, OC = outside corner.

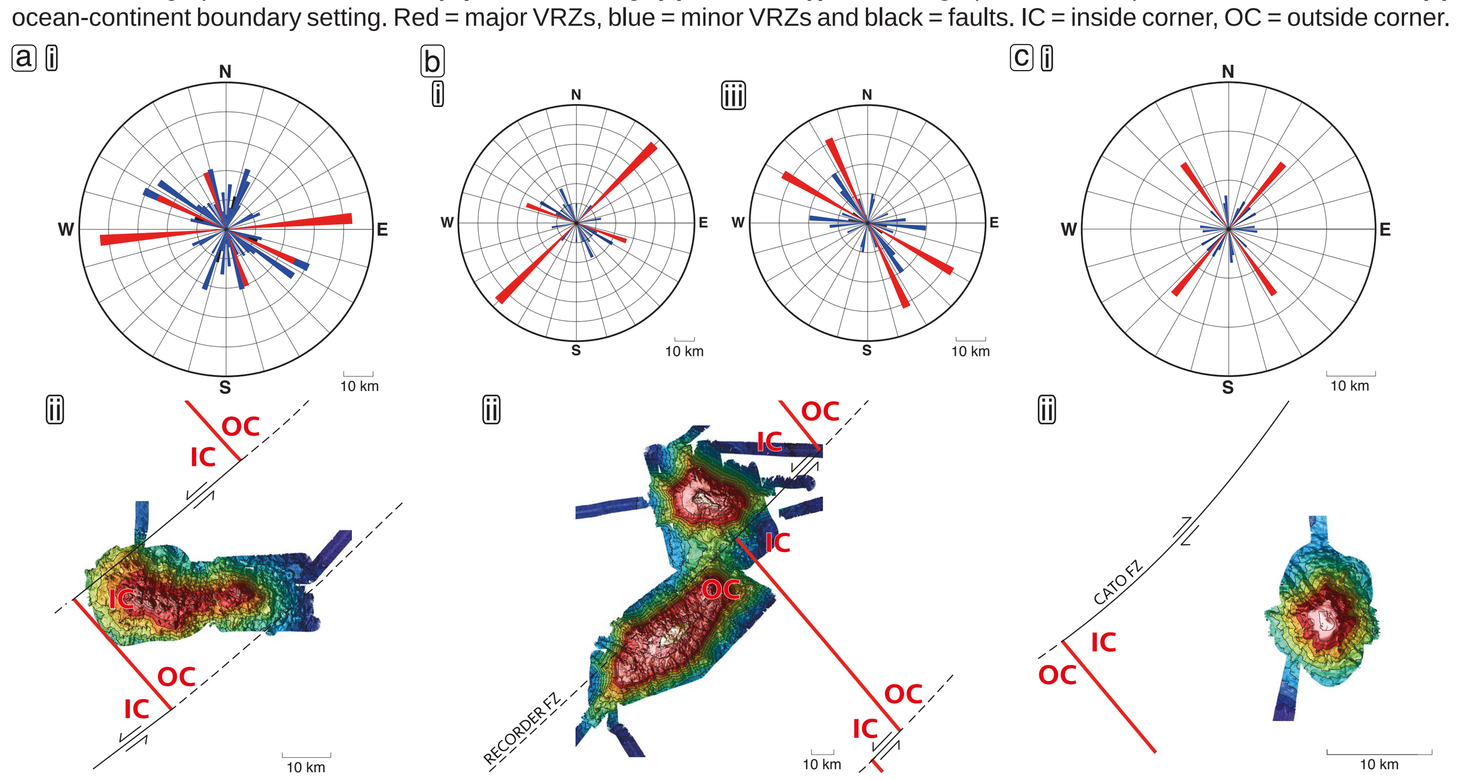

Figure 6. Linear feature orientations of all seamounts. **(a)** Axial ridges (red) and fracture zones (black). **(b)** Off-axis seamounts. **(c)** Fracture zone seamounts. **(d)** Inside corner seamounts. **(e)** Outside corner seamounts. **(f)** Continental seamounts.

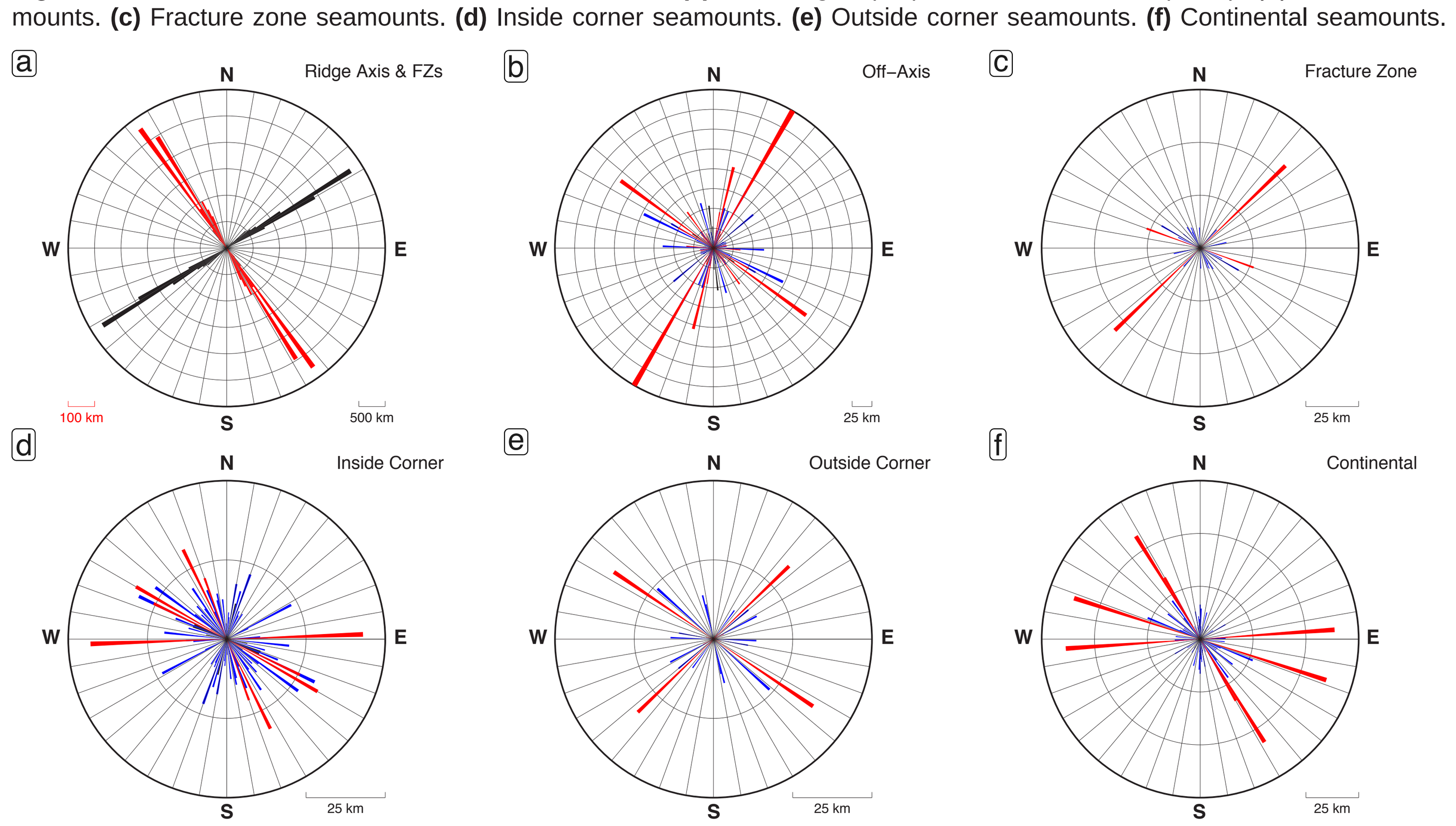

5 Deep Structure

- Bouguer anomalies are calculated by removing the combined gravity effect of the water-sediment and and sediment-seamount interfaces to investigate gravity signals related to deeper density interfaces.
- Calculations assume that seamount topography is uncompensated, i.e. the lithosphere is infinitely rigid.
- The reduction density of a seamount refers to the input seamount density that minimises spectral coherence between calculated Bouguer anomalies and the bathymetry.
- 20-50 mGal Bouguer highs over many seamounts, coupled with reduction densities up to ~3100 kg m^{-3}, suggest extensive intra-basement intrusion of primary magmas (cf. Contreras-Reyes *et al*., 2010).
- Low reduction densities over Cato and Wreck are consistent with both seamounts being emplaced on continental basement and significant fractionation of primary magmas (Hammer *et al*. 1990).

Seamount	Reduction Density (kg m^{-3})	Mean of Error (kg m^{-3})
Stradbroke	2760	12.5
Queensland & Britannia	2715	15.0
North & South Brisbane	3050	35.0
South Moreton	3135	30.0
North Moreton	2800	7.5
North & South Recorder	2805	37.5
South Fraser	2860	15.0
North Fraser	2825	60.0
Cato	2510	37.5
Wreck	2500	42.5

Table 1. Reduction density (i.e. seamount density, ρ_{sea}, that minimises weighted average coherence between gravity and bathymetry) for each of the Tasmantids with associated mean of error. Coherence and associated error are weighted using the power spectrum of the bathymetry.

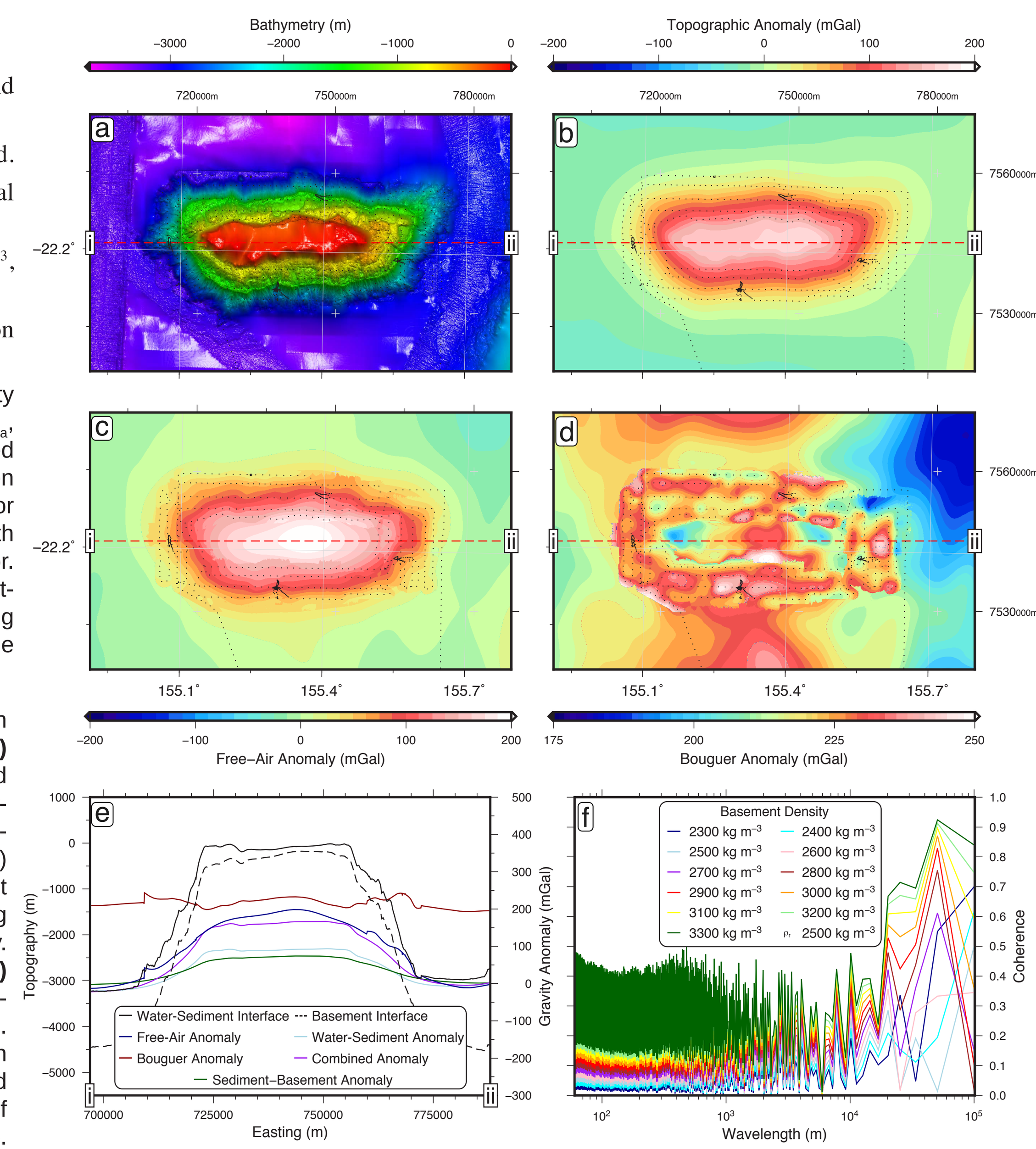

Figure 8. Gravity reduction over Wreck seamount. **(a)** Bathymetry. **(b)** Combined basement-seafloor interface topographic anomaly (sediment density (ρ_{sed}) = 2000 kg m^{-3}; seamount density (ρ_{sea}) = 2500 kg m^{-3}). **(c)** Free-air anomaly. **(d)** Bouguer anomaly. **(e)** Gravity anomaly and topography comparison. **(f)** Coherence between Bouguer anomaly and bathymetry for range of ρ_{sea} (2300 - 3300 kg m^{-3}).

- Alignments suggest deep faulting of the oceanic lithosphere allowing channelisation of magma along pre-existing structures despite emplacement post-dating active extension by >20 Ma.
- Dominance of the tectonic signal points to low melt production, implying that the Tasmantid "plume" was a relatively weak melting anomaly.
- Seamounts located at or adjacent to ridge-transform intersections have dominant trends oblique to spreading, implying strong mechanical coupling across the transforms.
- The high degree of mechanical coupling is consistent with slow Tasman Sea spreading rates and low rates of melt production.

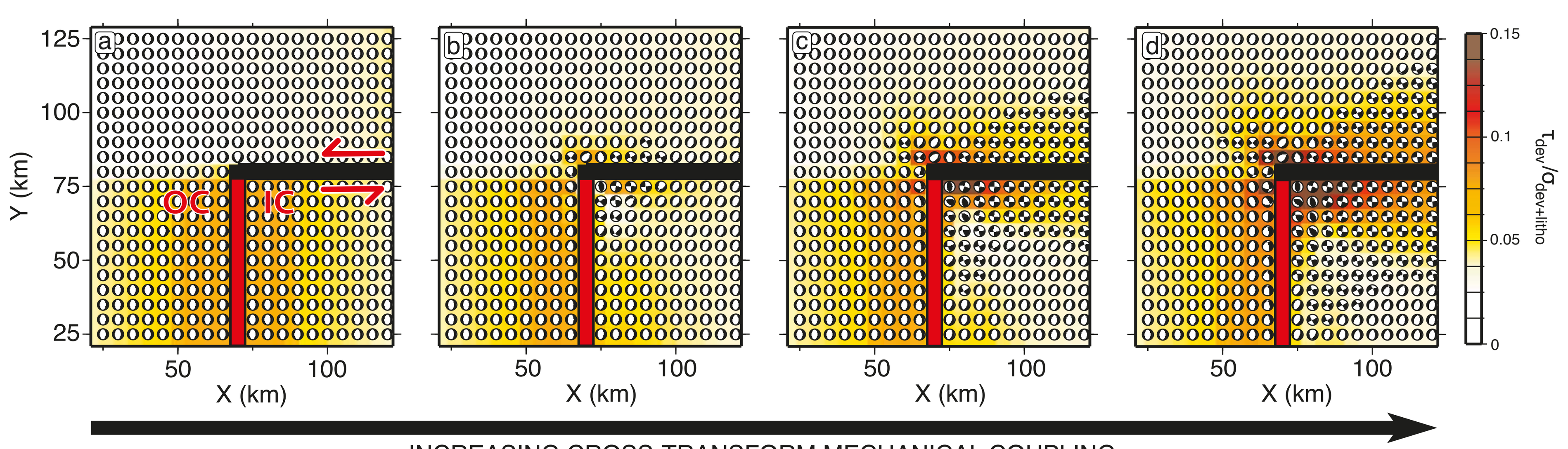

Figure 7. Effect of cross-transform mechanical coupling on principal stress orientations (modified after Behn *et al*., 2002). Focal mechanisms show optimal, calculated fault plane solutions at 4 km depth for differing degrees of mechanical coupling. χ = mechanical coupling, OC = inside corner, IC = outside corner, red = ridge axis, black = transform fault. $\tau_{dev}/\sigma_{dev+lith}$ is the ratio of shear to normal stress on the fault plane incorporating both deviatoric and lithostatic components. **(a)** χ = 0, **(b)** χ=0.05, **(c)** χ = 0.1 & **(d)** χ = 0.15. Horizontal displacement = 100m (10 ka at half-spreading rate of 1 cm a^{-1}).

6 Gravity Modelling to Determine Lithospheric Strength

- Models assume a finite-strength lithosphere and that the seamounts constitute loads, potentially associated with crustal roots and flexural moats.
- Inclusion of large sediment loads and extensive intra-basement intrusion of mafic magmas is required to achieve acceptable fits to observed gravity anomalies.
- There is no observable elastic thickness vs. age relationship along the chain.
- Seamounts emplaced at inside corners, fracture zones and on highly-extended continental basement have the lowest elastic thicknesses suggesting that structural inheritance, not age, is the dominant control on lithospheric strength.

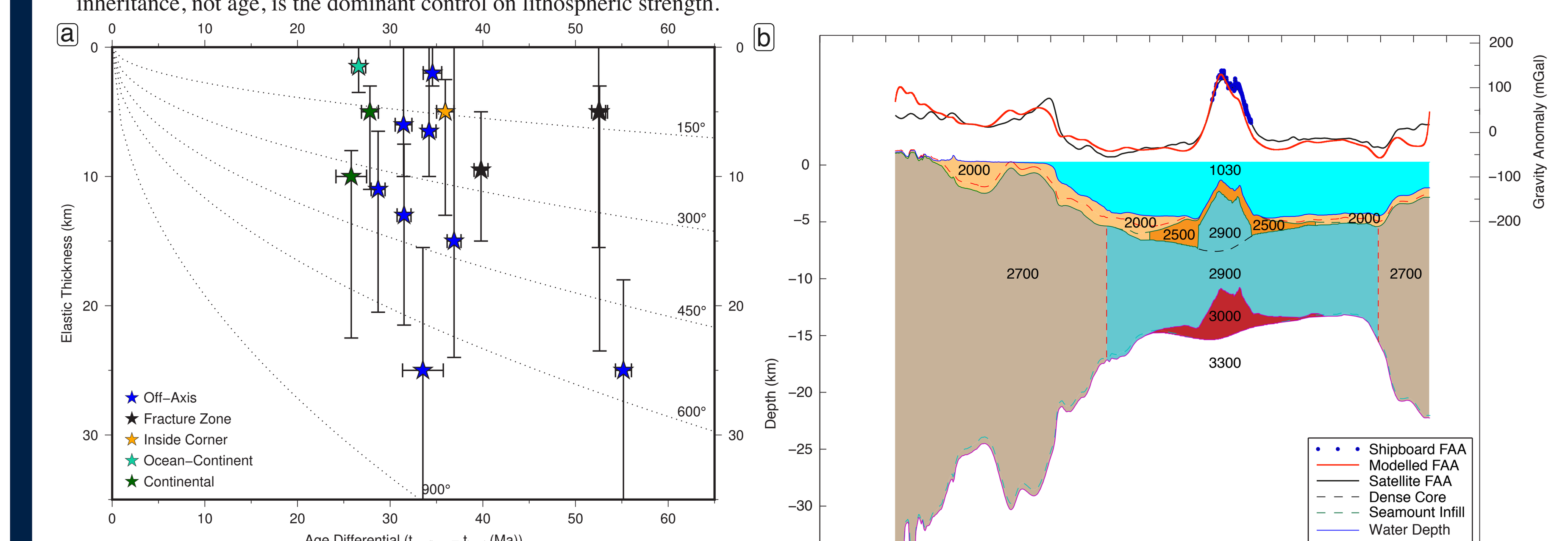

Figure 9. (a) Te vs. age of crust at time of loading with predicted isotherms for half-space plate cooling model. Data are coloured by tectonic context. **(b)** Best-fitting crustal model for Stradbrokeseamount from process-oriented gravity and flexure modelling. Values indicate densities (kg m^{-3}). TTS = Total Tectonic Subsidence.

7 Conclusions

1. The modest rates of mass wasting revealed by slope analysis, combined with the prevalence of dense cores indicated by gravity signatures and lithospheric modelling, suggest that subsurface intrusion, rather than sub-aqueous eruption, was the dominant magmatic growth mechanism.
2. Low overall Te and the >20 Ma time separation between seamount emplacement and spreading cessation suggest deep intra-lithospheric faulting must have accompanied spreading in order to allow Tasmantid magmas to exploit and align with pre-existing structural weaknesses.
3. Slow rate of magma supply, as indicated by the dominance of tectonic controls, high intrusive:extrusive ratios and scarcity of large mass-wasting deposits, points to a relatively weak Tasmantid melting anomaly.
4. Structural inheritance dominates the magmatic evolution of the Tasmantids as demonstrated by: i) dependence of morphology on tectonic setting; ii) lack of a Te-age relationship and iii) strong alignment of volcanic features with principal stress directions predicted for the Tasman Sea ridge system.
5. The strong dependence of intraplate magmatic fabric on extinct ridge structure demonstrates the importance of understanding tectonic inheritance and its influence on magmatic systems in both continental *and* oceanic settings.

References: **Beaman**, **2010**, MTSRF Project 2.5i.1a Final Report, pp. 13 & Appendix 1; **Behn** *et al*., **2002**, *Geophys. Res. Lett*., **29**(24), 2207; **Cohen** *et al*., **2013**, *Tectonics*, **32**, pp.1371–1383. **Contreras-Reyes** *et al*., **2010**, *EPSL*, **289**(3-4), pp. 323-333. **Hammer** e*t al*., **1990**, *Geophysics*, **56**(1), pp. 68–79. **Kalnins** *et al*., **2015**, **DI41A-2591**, *AGU Fall Meeting 2015*. **McDougall & Duncan** (1988), *Earth Plan. Sci. Lett*., **89**, pp. 207-220; **Mitchell** *et al*., **2002**, *Journ. Volc. & Geo. Res*., **155**(1-2), pp. 82–107; **Müller** *et al*., **2008**, *G³*,**9**, Q04006; **Ramalho** *et al*., **2013**, *Earth Sci. Rev*., **127**, pp.140–170; **Watts & Zhong**, **2000**, *Geophys. J. Int*., **142**, pp. 855-875.